Check for updates

Research Article | Vol. 31, No. 3 / 30 Jan 2023 / Optics Express 4122

Optics EXPRESS

Monitoring sidewall tilting of pixelated nanogratings in 3D display

CHAO CHEN,[1] XIUGUO CHEN,[1,4] SHENG SHENG,[1] ZHONGWEN XIA,[2] JIACHENG SHI,[2] WEN QIAO,[2,5] AND SHIYUAN LIU[1,3]

[1] *State Key Laboratory of Digital Manufacturing Equipment and Technology, Huazhong University of Science and Technology, Wuhan 430074, China*
[2] *School of Optoelectronic Science and Engineering & Collaborative Innovation Center of Suzhou Nano Science and Technology, Soochow University, Suzhou 215006, China*
[3] *Optics Valley Laboratory, Wuhan 430074, China*
[4] *xiuguochen@hust.edu.cn*
[5] *wqiao@suda.edu.cn*

Abstract: Sidewall tilting is an important parameter to describe the grating morphology and would affect the diffraction efficiency of three-dimensional (3D) display devices based on pixelated nanogratings. However, there is currently a lack of a non-destructive measurement method that can accurately measure the sidewall tilting of the pixelated nanogratings. This is mainly because the kind of nanograting is manufactured in a micron-scale pixel region and the grating lines generally have various directions to ensure that the display device can display images smoothly. In this work, we propose to use a home-made imaging Mueller matrix ellipsometer (IMME) to monitor sidewall tilting of pixelated nanogratings. Simulation and experiments were carried out to characterize the sidewall tilting angle. Through the combination of Mueller matrix elements, we can quickly and qualitatively identify the tilting angle for the purpose of on-line quality monitoring of the device. Through the inverse calculation of the Mueller matrix, we can accurately and quantitatively obtain the value of the tilting, so as to meet the demands of the device design. It is expected the proposed method can provide guidance for the identification and detection of tilting in 3D display elements based on pixelated gratings.

© 2023 Optica Publishing Group under the terms of the Optica Open Access Publishing Agreement

1. Introduction

Three-dimensional (3D) display technologies provide people with a new way of understanding and perceiving the world [1–3]. As one of the realization forms, the 3D display technology based on diffraction elements has always been considered as the one that may be commercialized the fastest because of its ability to obtain dynamic, color and three-dimensional display effects with a large field of view [4,5].

In order to increase the number of viewpoints and adjust the freedom of viewpoints to make the display smoother, Fattal D. [6] of Hewlett-Packard Labs proposed a diffractive 3D display scheme in the journal *Nature*. The structure is composed of pixelated nanogratings. At the same time, combined with LCD technology, the displayed viewing angle image pixels are matched with the nanograting pixels, and the direction of the light is adjusted by the nanostructure. The visual angle image is separated into different viewpoint positions to form a multi-viewpoint autostereoscopic display. To achieve a better display effect, the shape of the pixelated gratings needs to be purposefully designed.

As a modulation parameter of the pixelated grating's shape, the left and right sidewall angles also affect the display effect, to be precise, the diffraction efficiency of the device. Whether the two side wall angles are equal or not directly determines the tilting of the pixelated grating. The tilting of the pixelated grating is sometimes introduced artificially in the design, but it is also

#478503
Journal © 2023

https://doi.org/10.1364/OE.478503
Received 20 Oct 2022; revised 3 Jan 2023; accepted 4 Jan 2023; published 20 Jan 2023

possible that due to the limitations of the manufacturing process, the grating is not artificially introduced.

Currently, there are some non-destructive means to characterize the sidewall tilting of pixelated gratings with a micron-scale area size. Among them, the Mueller matrix ellipsometry is an important scientific instrument to analyze samples by using the polarization state change information of light. By using the 4×4 order Mueller matrix, rich information of the measured materials can be acquired, and then optical properties and morphology parameters can be analyzed and obtained [7–10]. There have been some studies on the measurement of sidewall tilting of nanostructures using the Mueller matrix ellipsometry [11–15]. For the angle-resolved Mueller matrix polarimeter, because the back focal plane imaging method is used, the polarization information will overlap in the back focal plane during measurement. This increases the difficulty of analysis. For other system without imaging process, limited by the resolution of the measurement system, these works are only applicable to samples large than the spot size.

Therefore, facing the measurement problem of the sidewall tilting of the pixelated nanograting in 3D display, we propose to use a home-made imaging Mueller matrix ellipsometer (IMME). In previous work, we have attempted to use IMME in the measurement study of pixelated gratings [16]. This work will serve as a further generalization of the previous work to rapidly qualitatively identify and accurately quantitatively characterize the sidewall tilting of pixelated gratings. This paper proceeds with the following content. In Section 2, the hardware configuration and performance of the IMME are introduced. In Section 3, the influences of the tilting on the Mueller matrix were simulated. At the same time, the influence of non-artificially introduced tilt on the display effect of 3D display is also studied. The paper is concluded in Section 4.

2. Experimental setup and method

Figure 1 shows the model diagram of the home-made imaging Mueller matrix ellipsometer [17]. The insert presents an overall view of the IMME. The system is made up of a light source module, a polarization state generator (PSG), a microscopic imaging module, a polarization state analyzer (PSA) and a detection module. The light source module is composed of a supercontinuum laser source (WhiteLase SC-400, NKT Photonics, Inc., Denmark), a monochromator (LLTF, NKT Photonics, Inc., Denmark) and an anti-speckle module. The PSG and PSA are both composed of a polarizer (PGT5012, Union Optics, Inc., China) and a self-designed super-achromatic composite waveplate (also called a compensator). The microscopic imaging module is composed of a high-numerical-aperture objective lens (OL, EC Epiplan - Apochromat 50 ×/ 0.95 HD DIC, Zeiss, Inc., Germany) and three doublet lenses (AC254 series, Thorlabs, Inc., USA). The detection module is composed of a detector (Andor Zyla 5.5, Oxford Instruments, Inc., UK). The system adopts a dual-rotating-compensator mode to detect the signal of the sample. All elements are well installed to avoid affecting imaging and ellipsometric accuracy.

The IMME can realize wide-field microscopic imaging measurement with sub-micron lateral resolution. The lateral resolution is better than 0.8 μm at full measurement band. Full Mueller matrix ellipsometric measurement can be realized, and all 16 Mueller matrix elements information corresponding to each pixel of the microscopic image can be obtained. Using air as the measurement sample, the accuracy of all Mueller matrix elements is better than ±0.005. The spectral measurement range that IMME can currently achieve is 410 nm −800 nm. It is worth noting that although the spot size of the instrument is about 150 μm, due to the imaging measurement method, even areas smaller than the spot size can be analyzed one by one. In addition, combined with different analysis methods, the IMME can realize the measurement of topographic features such as film thickness and nanostructure size, as well as optical properties such as optical constants, optical depolarization, and anisotropy.

Rigorous coupled-wave analysis (RCWA) is used to calculate theoretical Mueller matrices and diffraction efficiencies of the pixelated gratings [18,19]. The structure used is shown in

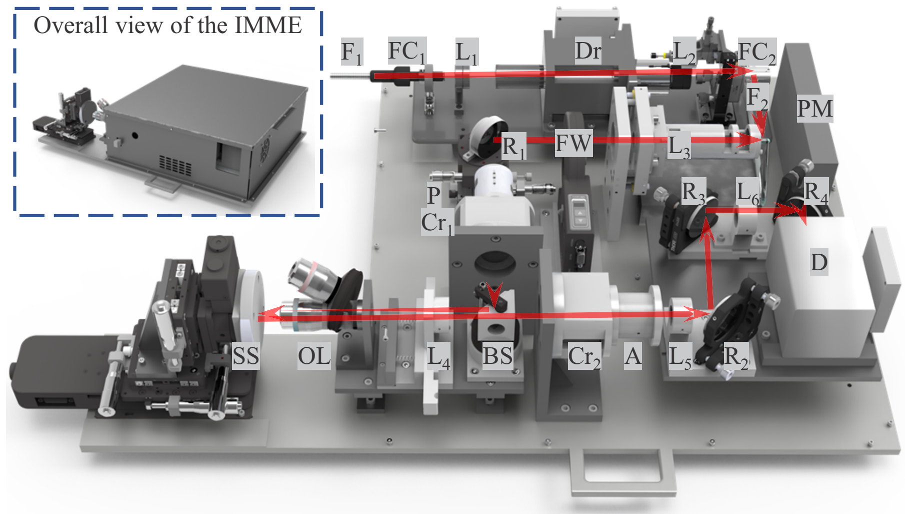

Fig. 1. Rendering of the home-made imaging Mueller matrix ellipsometer (IMME). F_1~F_2: fibers; FC_1~FC_2: fiber collimators; L_1~L_6: lenses; Dr: rotating diffuser; PM: power-supply module; FW: filter wheel; R_1~R_4: reflectors; P: polarizer; Cr_1~Cr_2: rotating compensators; BS: beam splitter; OL: objective lens; SS: sample stage; A: analyzer; D: detector. Insert: overall view of the IMME.

Fig. 2. The main consideration here is the detection of changes in the diffraction efficiency of the pixelated grating due to artificial or non-artificial tilting. The grating tilt δ_{swa} is defined mainly by the difference between the left and right sidewall angles, that is:

$$\delta_{swa} = \theta_{swa-L} - \theta_{swa-R}, \tag{1}$$

where θ_{swa-L} and θ_{swa-R} are the left and right side wall angles of the grating structure, respectively.

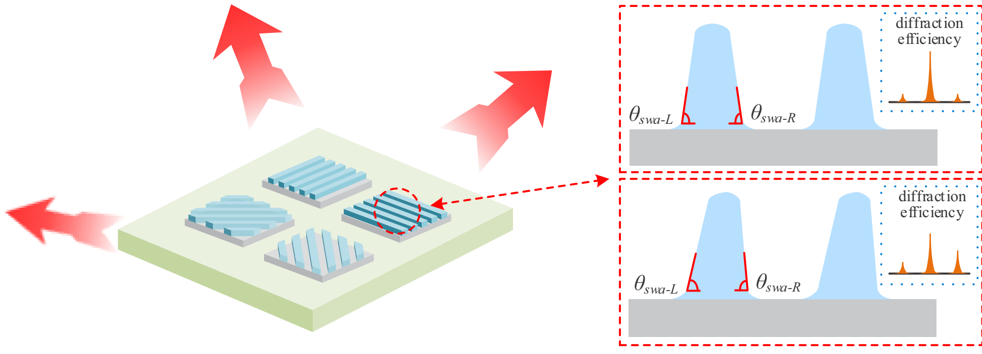

Fig. 2. Schematic diagram of the pixelated grating in 3D displays. The dashed boxes are the schematic cross-sectional views of the non-tilted and tilted grating morphology, respectively.

At the same time, the sum of the Mueller matrix elements $m_{13} + m_{31}$ (the range of the indices of Mueller matrix elements is 1-4) has a linear relationship with δ_{swa}, which can also be used to characterize the influence of the pixelated grating tilt on the diffraction efficiency [11].

$$m_{13} + m_{31} = c\delta_{swa} + b, \tag{2}$$

where c and b are constants.

3. Results and discussion

We simulated the Mueller matrices of grating structures with equal and unequal left and right sidewall angles, as shown in Fig. 3 to see whether the Mueller matrix is sensitive to the sidewall tilting. The duty ratio of the grating medium was 1:1. The period of the grating was set to 500 nm. The top critical dimension was 120 nm. The height of the grating was 180 nm. The situations where tilting angles are ±10°, 0° were considered ($\theta_{swa-L} = 50°$, $\theta_{swa-R} = 40°, 50°, 60°$). The wavelength was set to 450 ~700 nm, which is consistent with the measurement wavelength range of IMME. The angle of incidence was set to 60 degrees. The azimuth angle of the grating was set to 90 degrees. From the results, it can be seen that gratings with $\delta_{swa} = 0°$ can be quickly identified by setting the grating azimuth angle to 90°. Moreover, the Mueller matrix is very sensitive to such small angular changes, so it can be used as a tool to detect the sidewall tilting of the pixelated grating.

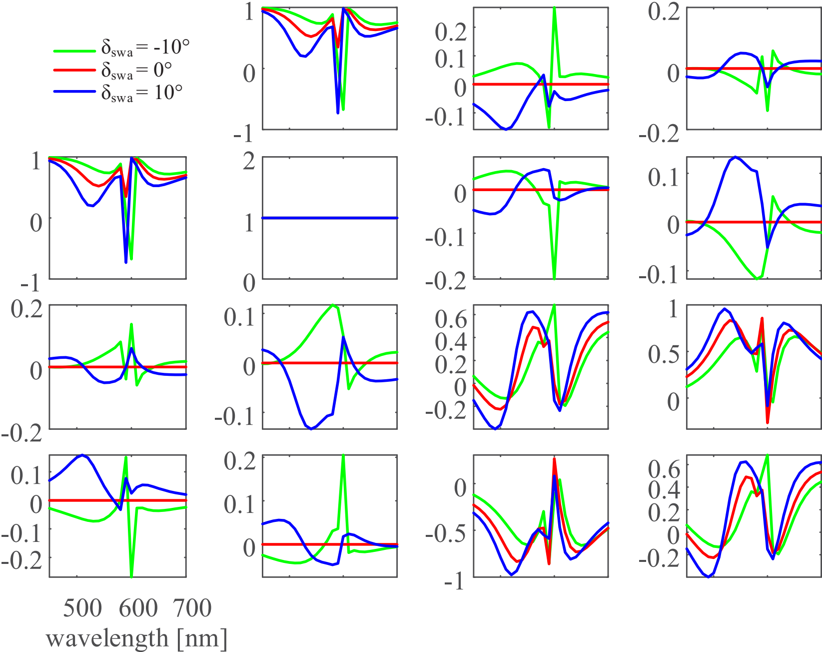

Fig. 3. Simulation results of Mueller matrices of grating structures with different δ_{swa}.

To demonstrate the ability of IMME to identify pixelated grating asymmetry in 3D displays, a sample containing 2400 grating regions was manufactured by spatial frequency variable photolithography (Nanocrystal 200, SVG Corporation) [20,21] developed by Soochow University. The material of the grating region of the sample is photoresist, and the substrate is quartz. The optical constants of the material have been accurately measured.

All regions have a size of 50 µm × 50µm and are closely spaced. Such distribution makes it difficult for traditional ellipsometry methods to collect the measurement signals of a single pixelated grating without interference from adjacent areas. The periods of the pixelated gratings are designed to be 500 nm - 550 nm, with an interval of 10 nm each. Each period of the grating is correspondingly designed with 10 orientations ranging from 0° to 90° at intervals of 10°. The shape of the grating is sinusoidal, and its left and right sidewall angles are set according to the same parameters. More sample information can be found in Supplement 1.

We measured all sample areas to study the tilting angles of the pixelated grating in the non-artificial case. The incidence angle is set to 60°. In order to quickly locate the position

Optics EXPRESS

of possible tilting, we fixed the azimuth angle at 90° when measuring the gratings. In order to verify the accuracy of this identification method, we fit the Mueller matrices of part of the gratings with the left and right sidewall angles set to the same and different. The results obtained by the instrument for the pixelated grating without sidewall tilting are consistent with those obtained by the scanning electron microscope, which can illustrate the accuracy of the instrument's measurement results. See Supplement 1. To be noted, we limited the aperture in the system so that only the 0th order diffracted light of the structure can be detected on the detector. Figure 4 shows one of the fitting results. As can be seen, when the left and right sidewall angles are set to be the same, the inverse model curves calculated by the RCWA method cannot match the measured results at all. However, when the constraint that the two sidewall angles are equal is removed from the model, it can be found that the curve produced by the model fits the measurement results well. From this aspect, it can be shown that the grating structure at this time has a certain tilting. This tilting is undesirable in the design because it affects the brightness and field of view of the 3D display structure. In addition, we can see that in the fitting cases under two different conditions, there are differences in the sensitivity to tilting of the main diagonal elements of the Mueller matrix and the off-diagonal elements. When there is a tilt in the structure, the off-diagonal elements can better reflect the accuracy of the fitting.

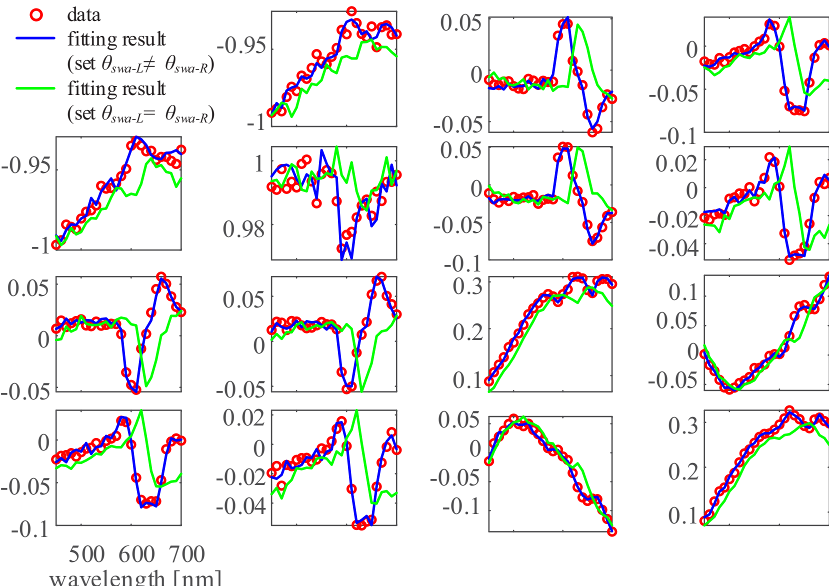

Fig. 4. Comparison between the pixelated grating fitting results under the condition of $\theta_{swa-L} \neq \theta_{swa-R}$ and $\theta_{swa-L} = \theta_{swa-R}$.

In addition, we also made statistics on the grating tilt on the sample, and verified whether there is a linear relationship between it and the Mueller matrix elements $m_{13} + m_{31}$. Part of Mueller matrix data can be found in Supplement 1. Figure 5(a) presents seven data points with sidewall tilting in the pixelated nanogratings with a period of 550 nm. The corresponding incidence wavelength is 600 nm, 530 nm and 450 nm, the incidence angle is 60°, and the azimuth angle of the grating is 10°. Figure 5(b) presents data points with sidewall tilting in the pixelated nanogratings with a period of 540 nm. The corresponding incidence wavelength is 600 nm, the incidence angle is 60°, and the azimuth angle of the grating is 70°, 50°, and 10°. There are clear linear relationships between several measurement data points. The mean square errors obtained

by the linear fitting are all large than 0.99. That is to say, $m_{13} + m_{31}$ has a certain relationship with the sidewall tilting of the grating structure.

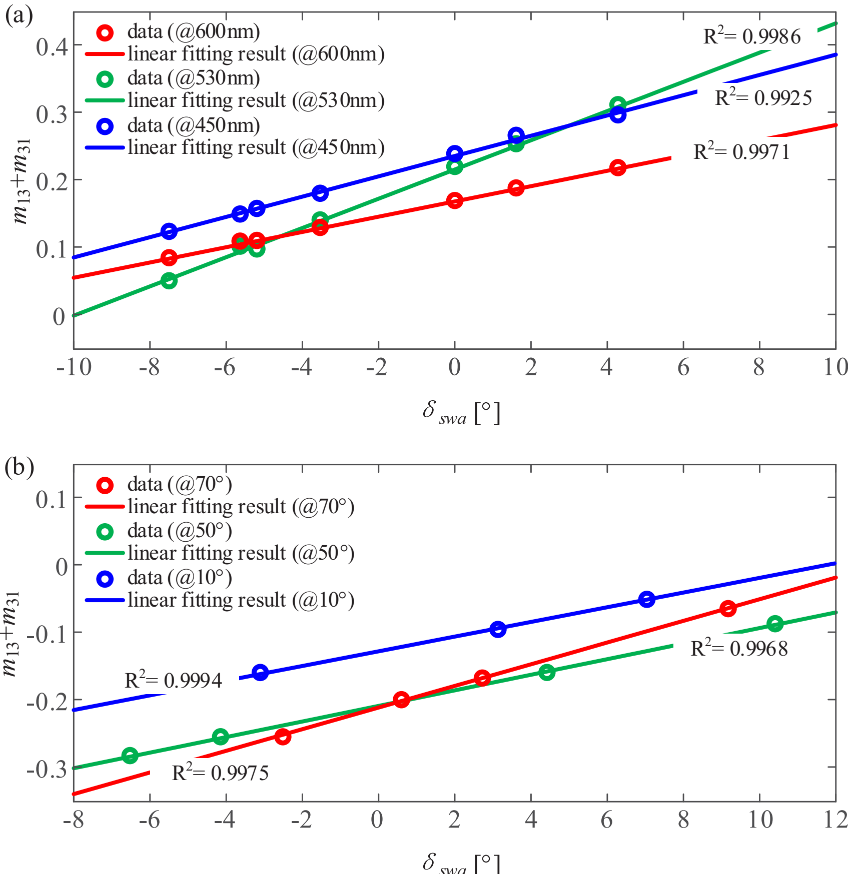

Fig. 5. The linear fitting results between $m_{13} + m_{31}$ and δ_{swa} at (a) different wavelengths and (b) different azimuth angles.

4. Conclusion

As a parameter that affects the diffraction efficiency of pixelated grating-based 3D display devices, the sidewall tilting needs to be monitored whether it is introduced by design artificially or by manufacturing errors. In this work, we propose to characterize the sidewall tilting of pixelated gratings by a home-made IMME. The IMME is not destructive to the sample and breaks through the limitation of the traditional ellipsometry method that the resolution is insufficient to meet the requirements of pixelated grating measurement.

In order to ensure the rapid online monitoring of the sidewall tilting of the device, we can qualitatively determine the sidewall tilting of the pixelated grating by combining the elements m_{13} and m_{31} of the Mueller matrix, and then obtain its diffraction efficiency. In order to guide the design of the pixel grating, we can obtain the values of the sidewall tilting through the inverse model based on RCWA. We verified the effect of the measured sidewall tilting on the Mueller matrix of the device through simulations and experiments. The method proposed in this paper also has certain limitations. For example, it is difficult to accurately obtain the signal of the tilt

angle when facing a structure with a high aspect ratio. The work is expected to provide guidance for the design and fabrication of 3D display elements based on pixelated gratings.

Funding. National Natural Science Foundation of China (52022034, 62175075, 51727809, 52130504); Key Research and Development Plan of Hubei Province (2020BAA008).

Disclosures. The authors declare that there are no conflicts of interest related to this article.

Data availability. Data underlying the results presented in this paper are not publicly available at this time but may be obtained from the authors upon reasonable request.

Supplemental document. See Supplement 1 for supporting content.

References

1. Z. C. Fan, Y. T. Weng, G. W. Chen, and H. E. Liao, "3D interactive surgical visualization system using mobile spatial information acquisition and autostereoscopic display," J. Biomed. Inform. **71**, 154–164 (2017).
2. D. Zhao, L. F. Ma, C. Ma, J. Tang, and H. E. Liao, "Floating autostereoscopic 3D display with multidimensional images for telesurgical visualization," Int. J. Comput. Assist. Radiol. Surg. **11**(2), 207–215 (2016).
3. J. Hua, D. Yi, W. Qiao, and L. Chen, "Multiview holographic 3D display based on blazed Fresnel DOE," Opt. Commun. **472**, 125829 (2020).
4. C. Y. Chen, Q. L. Deng, and H. C. Wu, "A high-brightness diffractive stereoscopic display technology," Displays **31**(4-5), 169–174 (2010).
5. Y. S. Hwang, F. K. Bruder, T. Fäcke, S. C. Kim, G. Walze, R. Hagen, and E. S. Kim, "Time-sequential autostereoscopic 3-D display with a novel directional backlight system based on volume-holographic optical elements," Opt. Express **22**(8), 9820–9838 (2014).
6. D. Fattal, Z. Peng, T. Tran, S. Vo, M. Fiorentino, J. Brug, and R. G. Beausoleil, "A multi-directional backlight for a wide-angle, glasses-free three-dimensional display," Nature **495**(7441), 348–351 (2013).
7. R. M. A. Azzam and N. M. Bashara, *Ellipsometry and Polarized Light*. (Amsterdam, 1977).
8. H. K. Tompkins and E. A. Irene, *Handbook of Ellipsometry*. (Sringer, 2005).
9. H. Fujiwara, *Spectroscopic Ellipsometry: Principles and Applications*. (Wiley, 2007).
10. X. Chen, H. Gu, J. Liu, C. Chen, and S. Liu, "Advanced Mueller matrix ellipsometry: Instrumentation and emerging applications," Sci. China Technol. Sci. **65**(9), 2007–2030 (2022).
11. X. Chen, C. Zhang, S. Liu, H. Jiang, Z. Ma, and Z. Xu, "Mueller matrix ellipsometric detection of profile asymmetry in nanoimprinted grating structures," J. Appl. Phys. **116**(19), 194305 (2014).
12. T. Novikova, P. Bulkin, V. Popov, B. H. Ibrahim, and A. Martino, "Mueller polarimetry as a tool for detecting asymmetry in diffraction grating profiles," J. Vac. Sci. Technol. B **29**(5), 051804 (2011).
13. C. Fallet, T. Novikova, M. Foldyna, S. Manhas, B. Haj Ibrahim, A. De Martino, C. Vannuffel, and C. Constancias, "Overlay measurements by Mueller polarimetry in back focal plane," J. Micro/Nanolith. MEMS MOEMS **10**(3), 033017 (2011).
14. J. Li, J. J. Hwu, Y. Liu, S. Rabello, Z. Liu, and J. Hu, "Mueller matrix measurement of asymmetric gratings," J. Micro/Nanolith. MEMS MOEMS **9**(4), 041305 (2010).
15. T. Novikova, A. De Martino, R. Ossikovski, and B. Drevillon, "Metrological applications of Mueller polarimetry in conical diffraction for overlay characterization in microelectronics," Eur. Phys. J. Appl. Phys. **31**(1), 63–69 (2005).
16. C. Chen, X. Chen, Z. Xia, J. Shi, S. Sheng, W. Qiao, and S. Liu, "Characterization of pixelated nanogratings in 3D holographic display by an imaging Mueller matrix ellipsometry," Opt. Lett. **47**(14), 3580–3583 (2022).
17. C. Chen, X. Chen, C. Wang, S. Sheng, L. Song, H. Gu, and S. Liu, "Imaging Mueller matrix ellipsometry with sub-micron resolution based on back focal plane scanning," Opt. Express **29**(20), 32712–32727 (2021).
18. M. G. Moharam, E. B. Grann, and D. A. Pommet, "Formulation for stable and efficient implementation of the rigorous coupled-wave analysis of binary gratings," J. Opt. Soc. Am. A **12**(5), 1068–1076 (1995).
19. L. Li, "Use of Fourier series in the analysis of discontinuous periodic structures," J. Opt. Soc. Am. A **13**(9), 1870–1876 (1996).
20. W. Wan, W. Qiao, W. Huang, M. Zhu, Z. Fang, and D. Pu, "Efficient fabrication method of nano-grating for 3D holographic display with full parallax views," Opt. Express **24**(6), 6203–6212 (2016).
21. Y. Ye, F. Xu, G. Wei, Y. Xu, D. Pu, and L. Chen, "Scalable Fourier transform system for instantly structured illumination in lithography," Opt. Lett. **42**(10), 1978–1981 (2017).

Supplemental Document

Optics EXPRESS

Monitoring sidewall tilting of pixelated nanogratings in 3D display: supplement

Chao Chen,[1] Xiuguo Chen,[1,4] Sheng Sheng,[1] Zhongwen Xia,[2] Jiacheng Shi,[2] Wen Qiao,[2,5,] and Shiyuan Liu[1,3]

[1] *State Key Laboratory of Digital Manufacturing Equipment and Technology, Huazhong University of Science and Technology, Wuhan 430074, China*
[2] *School of Optoelectronic Science and Engineering & Collaborative Innovation Center of Suzhou Nano Science and Technology, Soochow University, Suzhou 215006, China*
[3] *Optics Valley Laboratory, Wuhan 430074, China*
[4] *xiuguochen@hust.edu.cn*
[5] *wqiao@suda.edu.cn*

This supplement published with Optica Publishing Group on 20 January 2023 by The Authors under the terms of the Creative Commons Attribution 4.0 License in the format provided by the authors and unedited. Further distribution of this work must maintain attribution to the author(s) and the published article's title, journal citation, and DOI.

Supplement DOI: https://doi.org/10.6084/m9.figshare.21820131

Parent Article DOI: https://doi.org/10.1364/OE.478503

1 # Monitoring sidewall tilting of pixelated
2 nanogratings in 3D display

3

4 ## 1. Sample description

5 Figure S1 (a) shows the pixel area distribution of the measured samples. Figure S1 (b)
6 presents a scanning electron microscope image of one of the pixel gratings. The grating region
7 is mainly composed of three layers: the grating layer, residual adhesive layer, and substrate.
8 The shape of a sinusoidal grating is approximated as a trapezoidal grating. The optical constants
9 of the photoresists used are shown in the Fig. S2. Detailed model established for optical
10 constants fitting could be found in Ref. [1]. In order to obtain the grating topography accurately,
11 we approximate the grating topography with a multi-layer rectangle based on the strict coupled-
12 wave model. For gratings without sidewall tilting, we use top critical dimensions (*TCD*), line
13 heights (*H*), and sidewall angles to describe the topography. For gratings with sidewall tilting,
14 we use top critical dimensions, line heights, and left and right sidewall angles to describe the
15 topography. The established model is shown in Fig. S1 (c).

16

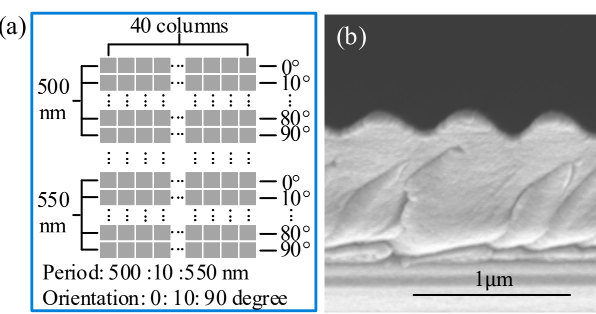

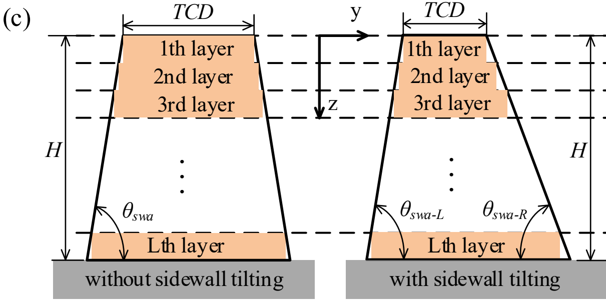

17

18 Fig. S1. (a) Schematic diagram of pixelated nanogratings; (b) the scanning electron microscope
19 image of the pixelated nanogratings; (c) schematic diagram of rigorously coupled wave
20 modeling for nanogratings with and without sidewall tilting.

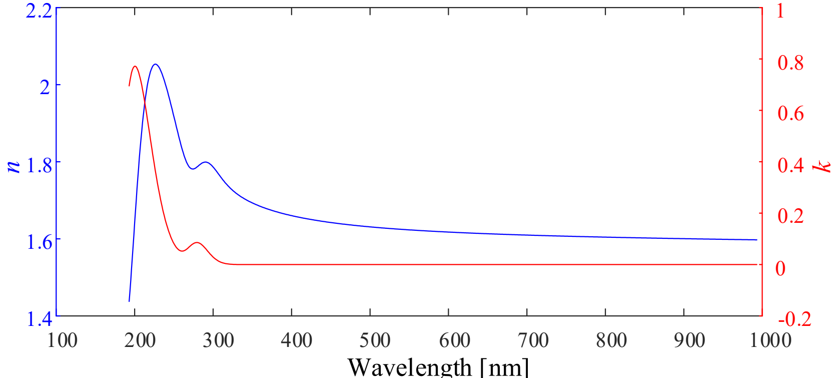

Fig. S2 Optical constants of the photoresist [1]

2. Inverse fitting results of the pixelated nanogratings

In order to verify whether the IMME measurement results are accurate, we fit the measurement spectra of some of the pixelated gratings and extract the parameters. Figure S3 shows the measurement results of the pixelated gratings with a period of 500nm at wavelengths of 450 – 700 nm. The measured incident angle was 60°. The measurement azimuths are 20° and 0°, respectively. The measured data at both azimuth angles can be accurately fitted to the model. The period is also fitted as a parameter to be solved, because when there is a difference between the period and the nominal value, it will affect the accuracy of the fitting result. Also, the left and right sidewall angles are set as two independent parameters to be fitted. We used the information at multiple wavelengths together as inputs to derive the topographical parameters of the measured structures [1]. Table S1 presents the extracted topographic parameters of the two pixelated gratings obtained by IMME from Fig. S3, and the results obtained by scanning electron microscopy. It can be seen that the results obtained by the two methods are consistent, which further illustrates the accuracy of the IMME.

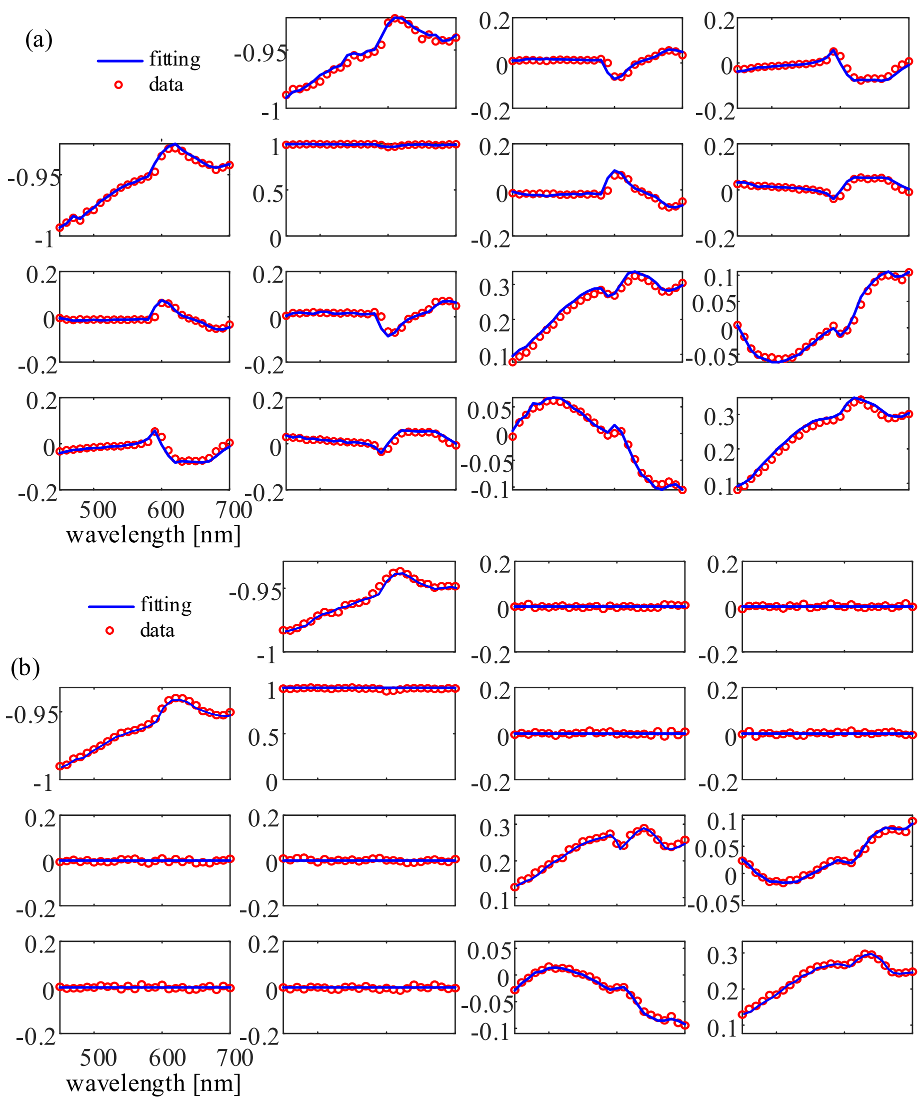

Fig. S3. Fitting results of pixelated gratings without sidewall tilting at azimuth angles of (a) 20° and (b) 0°.

Table S1. Parameter extraction results from IMME of the pixelated nanograting in Fig. S3 (95% confidence limits)

Parameters	IMME		SEM
	Azimuth-angle 20°	Azimuth-angle 0°	
Nominal Period (nm)	500	500	500
Period (nm)	498.1 ± 2.32	501.4 ± 3.58	501.1 ± 1.83
TCD (nm)	84.3 ± 0.67	85.3 ± 1.45	84.7 ± 1.15
H (nm)	180.5 ± 2.33	181.8± 3.66	183.1 ± 3.30
θ_{swa-L} (°)	53.3 ± 0.45	52.8 ± 0.77	54.0 ± 1.29
θ_{swa-R} (°)	53.4 ± 0.12	52.8 ± 0.23	53.8 ± 2.13

Taking a few data points as an example, Figs. S4-S7 show the Mueller matrix measurement and fitting results for the blue data points in Fig. 5 (b) and the red data point on the far right. It can be seen that the fitting effect is good. The extracted parameters are shown in Table S2.

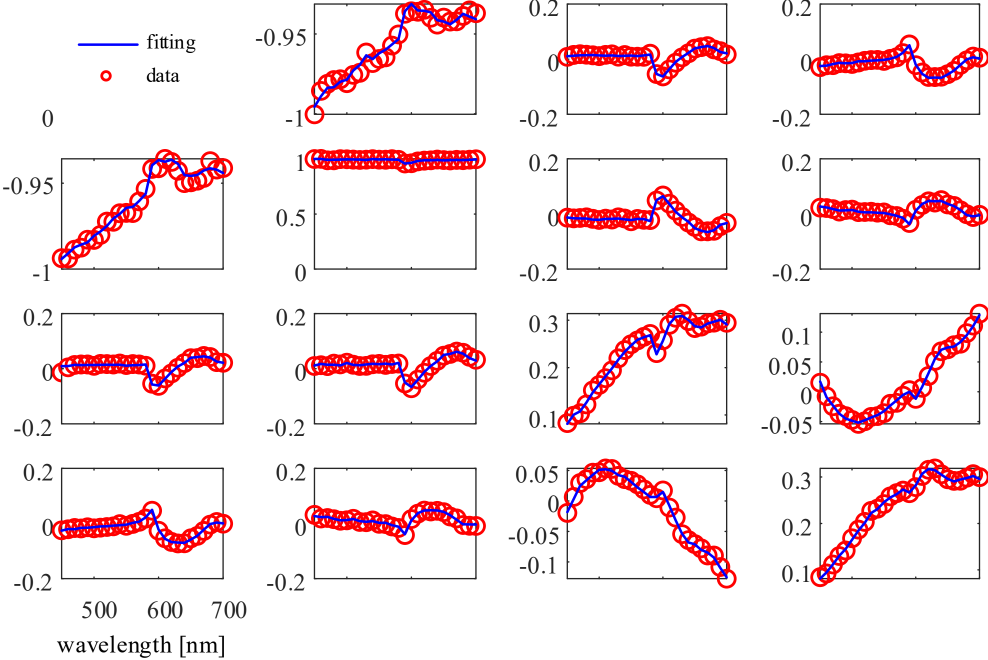

Fig. S4 Measurement and fitting results of the blue data point on the left in Fig. 5 (b).

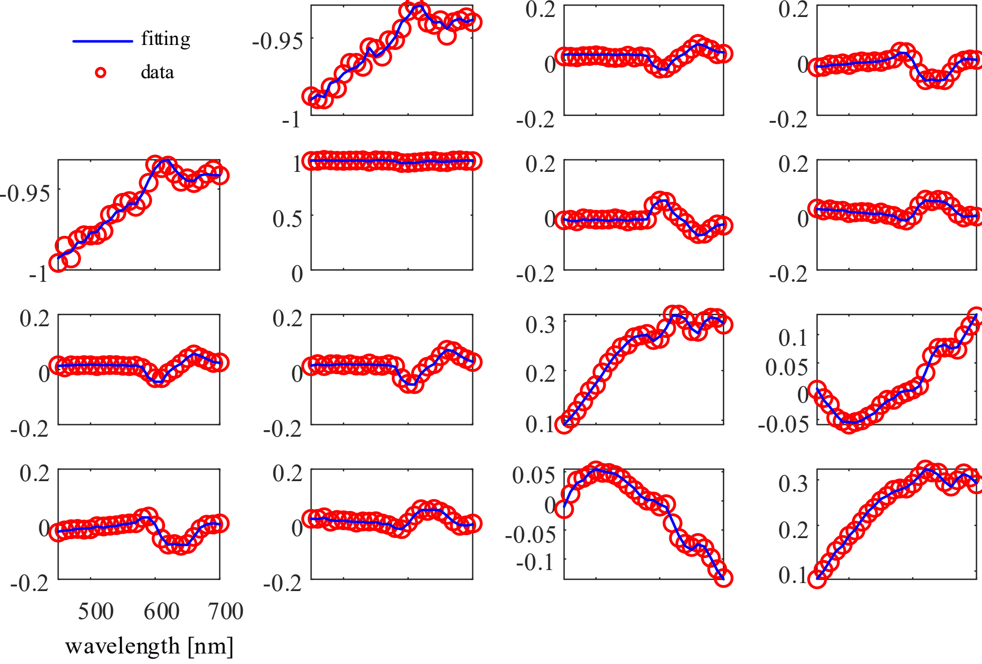

Fig. S5 Measurement and fitting results of the blue data point in the middle in Fig. 5 (b).

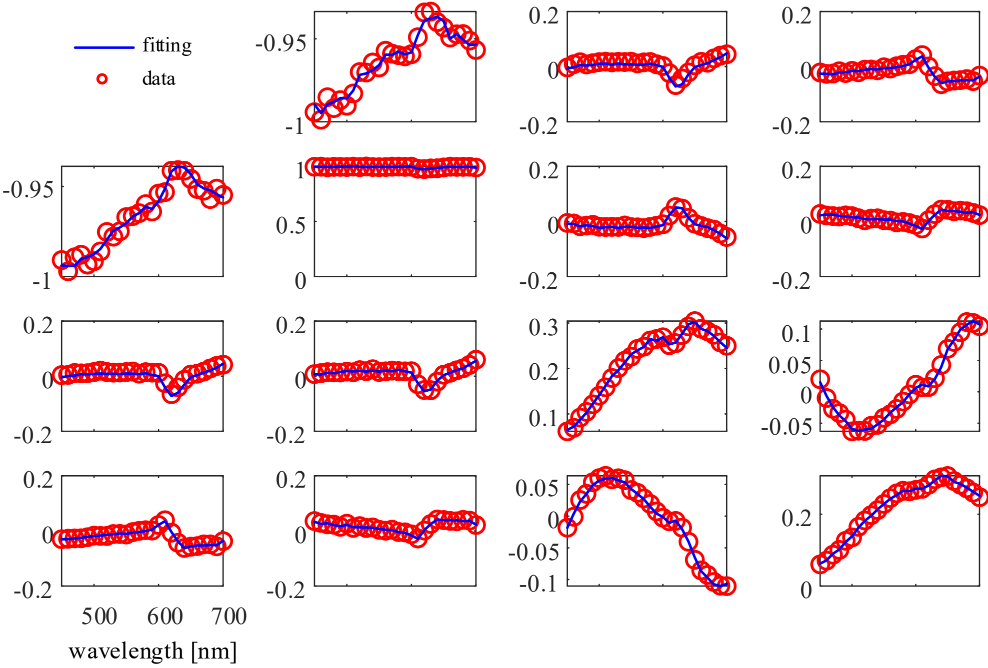

Fig. S6 Measurement and fitting results of the blue data point on the right in Fig. 5 (b).

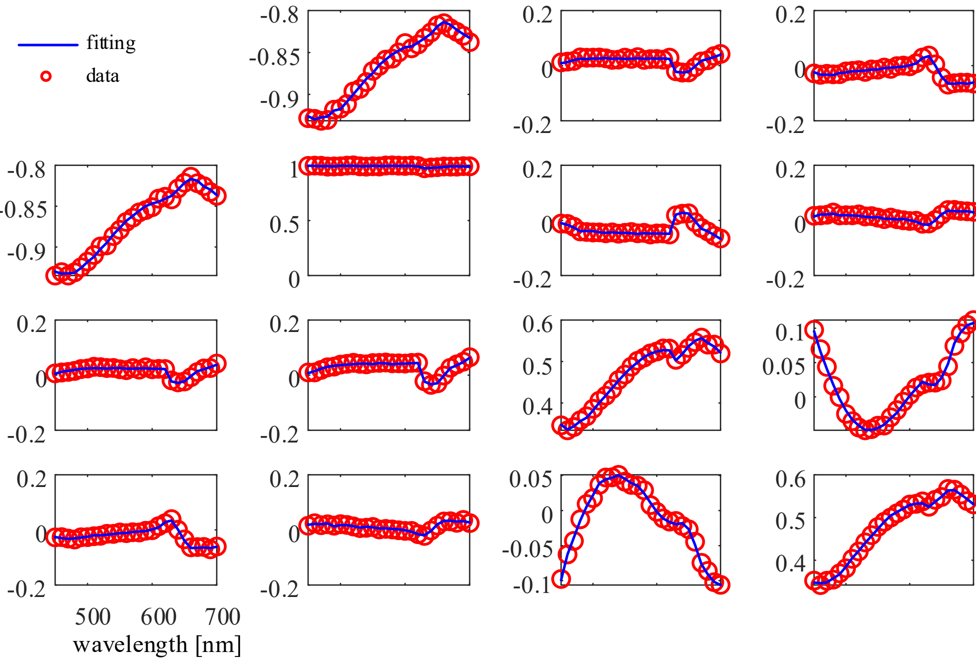

Fig. S7 Measurement and fitting results of the red data point on the right in Fig. 5 (b).

1 **Table S2. Parameter extraction results from IMME of the pixelated nanograting in Fig. S4-S7 (95%**
2 **confidence limits)**

Parameters	Point			
	Point in Fig. S3	Point in Fig. S4	Point in Fig. S5	Point in Fig. S6
Nominal Period (nm)	550	550	550	550
Period (nm)	547 ± 2.44	546 ± 2.71	552 ± 2.89	551 ± 1.89
TCD (nm)	91.8 ± 0.38	92.6 ± 1.64	94.2 ± 2.40	93.5 ± 2.91
H (nm)	179.6 ± 2.74	178.8 ± 2.87	178.5 ± 1.45	183.4 ± 2.72
θ_{swa-L} (°)	50.3 ± 0.29	56.2 ± 0.42	56.7 ± 0.37	54.6 ± 0.96
θ_{swa-R} (°)	53.4 ± 0.83	52.8 ± 1.26	49.3 ± 0.87	45.5 ± 0.10

3

4

5 **Reference**

6 [1] C. Chen, X. Chen, Z. Xia, J. Shi, S. Sheng, W. Qiao, and S. Liu, “Characterization of
7 pixelated nanogratings in 3D holographic display by an imaging Mueller matrix ellipsometry,”
8 Opt. Lett. 47, 3580-3583 (2022).
9 [2] C. Chen, X. Chen, Y. Shi, H. Gu, H. Jiang, and S. Liu, "Metrology of nanostructures by
10 tomographic Mueller-matrix scatterometry," Appl. Sci. **8**, 2583 (2018).